Development and Optimization of a Centrifugal Filtration Device for Small Samples

Pupo, Miguel[a]; Geraldes, Vitor[a]; Rodrigues, Miguel[a]

[a]Instituto Superior Técnico, Avenida Rovisco Pais, 1, 1049-001, Lisbon, Portugal

Abstract

Batchwise centrifugal filtration of small samples (<100 mL) for concentration of low molecular weight (MW < 1000 $g.mol^{-1}$) is process that was until recently thought to be unfeasible. Despite recent developments showing it's entirely possible to create a device capable of performing this operation, a commercial option still remains undeveloped.

This dissertation aims primarily at the creation of a commercially viable design for a device capable of performing this operation in an optimized manner. Secondarily, it aims at creating a device capable of performing ultrafiltration operations in a manner that is capable of dealing with protein adsorption and gel-layers formation near the surface of the membrane when non-saline solutions are used.

Such a device was created, with a modular system composed of a fixed base and removable membrane sample chamber was developed. This removable chamber allows for easier prototype preparation and retentate removal, better membrane cleaning and an all-round commercially improved filtration device.

With this device, fair permeate fluxes averaging 3.59 $mL.cm^{-2}.h^{-1}$ were obtained for ultrafiltration tests with a 5wt% solution of PEG35k. The rejection, despite averaging 80.63 % for initial tests where fissures allowed for solute permeation, was increase to 100% when such fissure formation was fixed.

Ultimately, the proposed design is innovative and presents a promising development for the field.

keywords: Centrifugal nanofiltration; Centrifugal ultrafiltration; Solute concentration; Non-saline protein solutions;

1. Introduction

Small-volume batchwise centrifugal filtration is a niche field within separation processes that offers a wide variety of applications, from cell filtration, body fluid compounds concentration and protein fractionization/concentration (Pall Life sciences 2003) to a wide variety of applications in pharmaceutical research (Lipnizki 2005; Székely et al. 2013). This process can easily substitute a plethora of other lab-scale separation processes (e.g. alcohol and salt precipitation, electrophoresis, dialysis, column chromatography, etc.) and it does so with versatility, low energy and cost requirements. Despite being able to only process small volumes (< 100 mL), this easily becomes an advantage when expensive solutes are used, or waste reduction is required. This is an already widely advance field, it is almost exclusively used for ultrafiltration and microfiltration (Baker 2000). However, recent years have shown some development in the field related to batchwise centrifugal nanofiltration (Completo et al. 2017; Hams 2018), which have shown this process is not only feasible, but highly marketable. Completo's design presented an aluminium device that was highly resistant to pressure and allowed for nanofiltration to occur and Hams approached the problem from a disposable point of view, attempting to create a prototype that could be discarded easily and cheaply.

While this process has shown promising, no commercial options exist yet to perform it. The current approaches were held together by either aluminium, which is expensive and not suited for disposable devices, or excessive amounts of glue, which are unsightly, difficult to work with and results in a lesser flux through the membrane. Even with ultrafiltration processes, highly optimized, several problems have appeared with the processing of proteins, specifically the formation of a gel layer or protein

adsorption at the membrane surface, which form when no salt is used in the solution and is rather difficult to clean (Porter 1972).
With all this in mind, this dissertation holds several objectives. First and foremost, it aims to create a functional centrifugal filtration apparatus that can operate at high pressures in order to perform nanofiltration based on a previous design by Hams 2018. Secondly, it aims to optimize said device with focus in minimizing mass transport limitation and functionality. Thirdly, it aims to make this prototype both more user-friendly and commercially viable.
As the project developed, the objective felt a change in direction, with the intention focussing in making a multi-functional device capable of multiple filtration events that range from microfiltration to nanofiltration. This device should be privy to all the limitations of the previous one and be able to function properly at different working conditions, as well as easily contradict protein gel layer formation.

1.1. Device performance

The performance of the device can be evaluated by analyzing two main parameters: Hydraulic permeability and solute permeability.
The former, hydraulic permeability (L_P), can be seen as an innate property of a new and fresh membrane (Porter 1990). It refers to the flux of pure water in said membrane per unit of transmembrane pressure and is therefore highly related to the pure water permeate flux, J_w, given by:

$$J_w = \frac{Q_w}{A_m} \quad (1)$$

where Q_w is the volumetric water flow and A_m is the membrane area. L_p can then be calculated by factoring in the transmembrane pressure.

$$L_p = \frac{J_w}{\Delta p_m} \quad (2)$$

Because the pressure gradient is the driving force that induces water movement from one side of the membrane to the other, the water flux is expected to increase with added transmembrane pressure. As such, L_p gives us an unbiased look at the flow through any particular membrane, regardless of the pressure used.
Using L_p it's also possible to calculate the membrane's resistance to water permeation, R_m (Carman 1997):

$$R_m = \frac{1}{\mu_w . L_p} \quad (3)$$

where μ_w is the dynamic viscosity of pure water. As the resistance increases with fouling, we can expect L_p to decrease with use. This explains why L_p of a membrane is always calculated for pristine membranes (Rudie, Torgrimson, and Spatz 1985).
As for solute permeability, it allows us a glimpse into the membrane's efficiency and selectivity. A good measure of this parameter can be obtained by measuring rejection coefficients.
Apparent rejection (R_a), otherwise known as observable rejection, is defined as the percentage of solute retained above the membrane:

$$R_a = \frac{c_f - c_p}{c_f} = 1 - \frac{c_p}{c_f} \quad (4)$$

where c_f and c_p are the solute concentration of feed stream and permeate stream. Any given membrane working under the size exclusion principle can be characterized by a molecular weight cut-off point (MWCO), which corresponds to the molecular weight for which the rejection will be 90%.

1.2. Mass transport through the membrane

Dead-end filtration requires a comprehensive knowledge of mass transport phenomena through the membrane layer. A multitude of models have been created to properly describe the inner workings of membrane processes.
The simplest model to deal with membrane filtration was the one selected for this work. The osmotic pressure model as laid out by Kedem and Katchalsky 1961, relates the solvent flux through the membrane and the effective pressure difference (Δp_{eff}).

$$J_v = L_P . \Delta p_{eff} \quad (5)$$

Δp_{eff} is a pressure-driven force between the active side (inhere after symbolised as m) and permeate side (inhere after symbolised as p) and can be calculated as $\Delta p_{eff} = p_{eff,m} - p_{eff,p}$. Δp_{eff} as considers both applied pressure (p) and osmotic pressure (π), such that

$$p_{eff,m} = p_m - \pi_m$$
$$p_{eff,p} = p_p - \pi_p \quad (6)$$

Considering $\Delta p_m = p_m - p_p$ and $\Delta \pi_m = \pi_m - \pi_p$, equation (2-6) can be re-written as

$$J_v = L_P.(\Delta p_m - \Delta \pi_m) \quad (7)$$

The osmotic pressure can be calculated using Lewis's equation (Lewis 1908)

$$\pi = \frac{R.T}{V_w}.\left(\frac{N}{1-N}\right) \quad (8)$$

1.3. Mass transport limitations

Under ideal conditions, the membrane layer would be the only resistance the fluid finds during the filtration process. However, in real processes, the mass transport becomes limited by several phenomena that need to be mitigated in order to ensure the optimization of any given process. For the present work, four phenomena have shown particularly problematic.

Fouling is a deposit of unwanted matter to build up over time on the membrane surface and/or within the pores due to continuous or repetitive use of a membrane (Ao et al. 2016).

Gel polymerization is most prominent in UF processes involving proteins and poly saccharides, where gelling can occur through rheological changes (Barr and White 2006) as well precipitation due to high applied pressure increasing solute concentration above the membrane

Compaction refers to the irreversible compression of a membrane under excessive pressure (Volkov 2014).

When pressure is exerted over a membrane during filtration, there is a tendency for particles to be pushed against the membrane surface and accumulate around it, limiting mass transfer. In porous membranes, this leads to pores being plugged, while compact ones felt diffusion resistance. This phenomenon is more widely known as Concentration Polarization (CP) (Luis 2018).

These phenomena collectively impede mass transport and have decrease flux, thus decreasing rejection and the overall performing
of the device.

Though several methods have been employed to mitigate these effects, such as static mixers, feed pacers, pulsating flow or irregular feed path, but the one explored in this work, centrifugal filtration, has proven particularly effective to this effect (Hilal et al. 2005).

1.4. Centrifugal filtration

Centrifugal filtration, dissected to its simplest terms, is the rotation of a filtration device around an axis. This rotation generates the main driving force of the process, a transmembrane pressure difference.

Although both sides of the membrane are exposed to atmospheric pressure, the fluid above the membrane, while it is in rotation, exerts enough hydrostatic pressure above the membrane to allow permeation (Svarovsky 2001). This pressure can be calculated thusly:

Consider an incompressible fluid element, dV, of mass dm. At a position r away from the rotation axis (rotating with constant angular velocity ω), this element will exert a pressure dP above the membrane (Figure 1).

$$dp = \rho.\omega^2.r.dr \quad (9)$$

If we consider the limits of the fluid element as r1 and r2, then the pressure difference generated is calculated as:

$$\Delta p = \int_{r_1}^{r_2} dp = \quad (10)$$
$$= \rho.\omega^2.(r_2^2 - r_1^2)$$

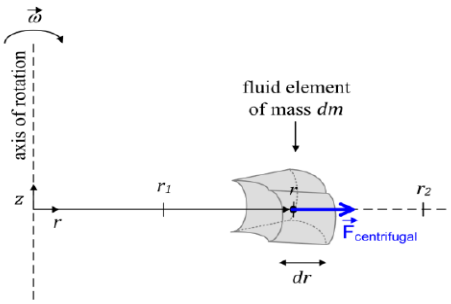

Figure 1 - Lateral view of a fluid element rotating around an axis (Completo 2018)

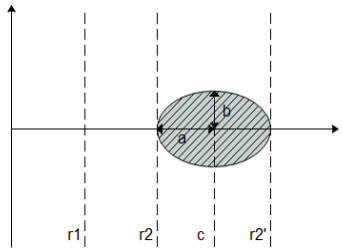

Figure 2 - Sketch of positions of interest on the centrifugal device. R1 is the liquid meniscus, r2 and r2' are the edges of the membrane and c is its centre.

Since these devices tend to have an angle, the pressure measurement varies from one edge of the membrane to the other. In addition, the pressure drops during filtration due to a reduced fluid volume. As such, all processes for these devices are characterized by the average pressure over the membrane on the initial point of filtration, $\overline{p_0}$, which can be calculated by integrating equation 2-18 over the membrane area (Figure 2).

$$\overline{p_0} = \frac{\iint_{A_m} \Delta p . dA}{\iint_{A_m} dA} \qquad (11)$$

Although a pressure difference would be enough to allow filtration, if this compression force was the only force present the particles would be squished heavily against the membrane and create the before mentioned mass transport limitations. So, where does this so called "Self-cleaning mechanism" come from. The answer lies in the existence of centrifugal and Coriolis forces, as calculated by:

$$d\vec{F}_{centr} = -dm \times \vec{\omega} \times (\vec{\omega} \times \vec{r}) \qquad (12)$$

$$d\vec{F}_{Coriolis} = -2.dm \times \vec{\omega} \times \vec{U} \qquad (13)$$

Centrifugal Force refers to the force dragging the fluid element away from the axis of rotation, and the Coriolis force refers to the fictional force that describes the actual movement of the fluid element. Since these forces are linearly dependent to the mass of the element, heavier particles will succumb to a larger effect, meaning if the membrane is angled away from the angle of rotation, the solutes will tend to be swept away from the membrane surface, allaying CP and fouling. Since these forces are much larger than the force of gravity, this becomes negligible and the particles are mainly dragged by the rotational movement. Calculating how negligible gravity is when compared to the centrifugal force can be done by using the rotational centrifugal force parameter (RCF):

$$RCF = \frac{centrifugal\ force}{gravitational\ force} = \frac{r.(2\pi.RPM)^2}{60.g} \qquad (14)$$

Utilizing this principle, there are two main things that can be recovered from a filtration process. The first is the permeate, clear of solute. The second is the retentate, rich in solute. The one of most interest for the device being created for this dissertation is the later.

Since concentrating a retentate is the main purpose, a parameter was used to determine how rich in solute it can become, the concentration factor CF, defined as the ration between the concentration of the permeate and the concentration of the feed

$$CF = \frac{c_r}{c_f} \qquad (15)$$

2. Prototype development

2.1. Methods

Apart from the device's outer shell, all the parts required were manufactured in Smartfil Polylactic acid filament (Smartfill 2019) using a Ultimaker 2+ 3d printer. The layer height selected was of 0.05 mm so as not to allow permeation of water into the device. The models were designed using a mixture of *Onshape* (Present Onshape Inc. 2014) and *Blender* (version 2.8; Blender foundation 2019) and sliced using *Ultimaker Cura* (version 4.3; Ultimaker 2019).

The membranes used for the device were the NF-90 (Filmtech 2019) and the FS40PP (Alfa Laval 2019).

The glues used were a 2-part epoxy, Zap® Z-Poxy 30 minute formula (Pacer Technology 2019) for the first test, and a cyanoacrylate gel, Loctite super flex (Henkel 2019), from the point

problems with PLA hydration and epoxy connections arose.

To test the performance of the prototypes, tests were performed at different pressure conditions at 20ºC in a Sorval RC 6 plus Superspeed Centrifuge (Thermo-Scientific 2019a) using a Thermo-Scientific SA-300 fixed angle rotor (Thermo-Scientific 2019b), at a 34º angle (α). The devices were positioned in such a way that β=0º, tested one at a time and counterbalanced using a water filled tube, deviating no more than 0.1g from the device, as specified by the centrifuge specifications In order to avoid the actions of the Archimedes' screw like lift inside the tube, which could de-stabilize the tube through turbulent forces and cause leaks, the acceleration and deceleration of the centrifuge were set to three minutes each. Due to the variations in rotor velocity (limited by the centrifuge), all pressures herein are given the name of nominal pressure and are understood to hold a variation of up to 5%.

The tests used pure water for both NF and UF and binary aqueous solutions containing Coomassie brilliant blue G-250 (Sigma-Aldrich 2019a) and polyethylene glycol 35k (Sigma-Aldrich 2019b) for NF and UF tests, respectively. The G-250, with a MW of 854 $g.mol^{-1}$, was prepared by diluting 0.025g of the solute in 100.0 mL of unionized water (conductivity lower than 5 $\mu S.cm^{-1}$), in order to wield a negligible osmotic pressure ($\pi_f < 10^{-2}$ bar). The PEG 35k was prepared by diluting 5.360 g in 100.0 mL of unionized water for a 5.0 wt% solution with $\pi_f = 3.7 \times 10^{-2}$ bar.

Unless otherwise stated, the membranes were cleaned using a Ultrasil 110 (Lenntech 2001) dilute solution, carefully scrubbed with a cotton bud and centrifuged with unionized water at 5 bar for 20 minutes.

2.2. Device design

The devices used all present with the same basic structure. Following the designs of Completo et al. (2017) and Hams (2018), the devices used are composed of a shell, a lid and a membrane support.

The shell , composed of polycarbonate (Hams 2018), serves to envelop the functional parts of the device. Made from a 50 mL Nalgene round centrifuge tube (Thermo scientific 2001), this tube was fitted with a 1.6 mm hole 23.0 mm from the bottom in order to alleviate pressure during filtration on the permeate side and to easily remove permeate with aid of a syringe.

The lid has a cork-like design, with a lower part that goes into the shell and an upper part that stops the lid from entering further. This top part is ridged to facilitate removal, as it makes it easier to grip. A hole goes through the lid in order to normalise pressure from the retentate side. This hole, 9mm from the centre of the lid, has a conical design with a diameter of 1.5 mm on the top but only 0.4 mm at the bottom. This design, through the action of capillary forces, makes it difficult for fluid to flow through this hole and minimizes leaks from the retentate side.

The membrane support has the function of keeping the device structurally sound. As such, it needs to be able to sustain any forces. While tensile forces aren't an issue with the current device, the design needed to account for the action of shear and compressive forces. This support column was designed with a 25 mm support strut. This translates into a maximum allowed permeate volume of 5.2 mL for this design. This conical approach therefore optimizes the previous allowed permeate volume of 2.3 mL (Hams 2018).

Additionally, in order to facilitate gluing further, instead of a net-like support beneath the membrane like used on previous trials, the membrane support for this dissertation was modelled with inbuilt ridges, emulating this net and allowing permeation by stopping the membrane from being compressed against the support surface.

The axial positions of interest for this design are r2 = 54.7 mm and r2' = 83.0 mm.

2.3. Experimental Prototype development

Several different designs were tested. The most important designs developed throughout this work are detailed here

2.3.1. Sealed chamber trials

The point of the first performance test was to determine if sealing was possible with a reduced amount of glue. Hams' prototype (Hams 2018) was selected, slightly altered to better suit commercial applications. Firstly, a 2.0 mm ring, 0.6 mm thickness, was fitted above the

membrane, which both homogenizes the glue and levels the membrane surface. Secondly, the glue amount was vastly reduced and kept only on the sides of the support, so as not de-stabilize the membrane surface. This model was then fully sealed with epoxy instead of being fitted with a membrane.
The device was tested at different velocities with increments of 1000 rpm starting at 5000 rpm. A G-250 solution was used as a tracer for better visibility and leak detection. The results show that no liquid permeate the device up to 18000 rpm, corresponding to a pressure of 66 bar, showing that the device should remain sealed at working conditions of up to 30 bar.

2.3.2. Open chamber trials

Using the same model as the previous trial, this time fitted with a NF membrane, one wanted to test the pure water permeation of the device. For this purpose, 10 and 20 mL of tracer solution of G-250 were filtered using two similar devices at different pressures at 5 bar intervals. Different filtration times were used to avoid overflowing the chamber. The results are detailed bellow. Since the rejections were evaluated on a purely visual basis, no value is given.

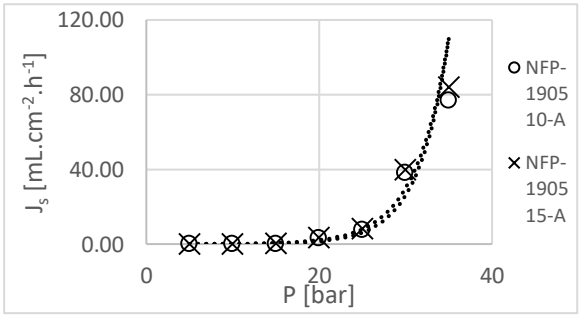

Figure 3 - Open chamber result graph: Water flux tests in prototypes NFP – 190510 – A and NFP – 190515 – A.

Here, we expected to see a linear relationship of Flux with relation to pressure. However, the relationship observed shows an exponential behaviour, starting at around 25 bar, pressure at which blue dye became visible in the permeate. Further tests using the same devices verified that, after the previous tests, flux at 10 bar had highly increased and blue dye permeated. It's therefore safe to assume pressures higher than 20 bar damage the gluing of the current device beyond fixability, allowing permeation of the tracer dye through the gaps in the glue.
Further dissection of the membrane concluded that the gluing problem occurred on the membrane-PLA connections for smaller pressure (<30) bar. This was determined by the presence of a blue ring around the membrane on its bottom side, showing that the permeation was through the sides rather than through the membrane. The massive increase in flux from 30 bar onwards is explained by the blue line found from this point on around the membrane support and shows that the gluing needs to be optimized not just for membrane-PLA connections, but also for the PLA-PC connections, that cannot handle high pressures. This is, presumably, because the PC expands at a different rate than the PLA, causing tension to build up in the glue.
A secondary theory states that as the PLA hydrates, it connects less and less to the epoxy glue, meaning that the more tests performed, the worse the connection becomes. As PLA is somehow permeable to water (Siparsky et al. 1997), despite the printing properties chosen (layer height, printing speed, filling shape and density) minimizing the effect (Gordeev, Galushko, and Ananikov 2018; Stansbury and Idacavage 2016), it hydrates. It appears hydrated PLA affects its connection to epoxy glue and is therefore not as optimal for this particular application as thought before. This is the reason a cyanoacrylate was used hereafter.

2.3.3. Modular system trial

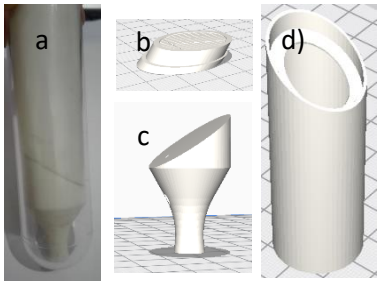

Figure 4 - Several views of the modular device a) Side view of printed device; Cura view of b) membrane support part, c) module support part and d) Module part.

Derived from the previous tests, this idea relies on the principle that PLA-PC connections are wildly flawed. As such, a device was designed that connected the membrane to a PLA tube directly, leaving the support to a separate piece and eliminating the need for the PLA-PC connection entirely (Figure 3).

Despite having similar conditions, the results of these tests vary wildly. The flux varies between 2.134 ± 0.004 mL.cm^{-2}.h^{-1} and 4.472 ± 0.005 mL.cm^{-2}.h^{-1}. We can easily blame the differences in L_p for this, as due to the small membrane areas being used, there will be sufficient differences in both the number and shape of pores and in the matrix of the membrane to cause significant variation.

As for the rejection, it varies between 65.194±0.008 % and 87.95±0.03 %, averaging 80.63±0.02 %. Compared to the expected rejection for solute with the MW of PEG35k of around 100%, these results show that leaks must have occurred in every device. By observing Figure 4, a linear upwards trend becomes visible with relation to J_s. This relationship was predicted by the mass transfer models and shows that the bulk of the flow was through the membrane, meaning any leaks must be due to small imperfections in the gluing. This is confirmed by the fact that the fluxes fall within the expected order of magnitude for the membrane used.

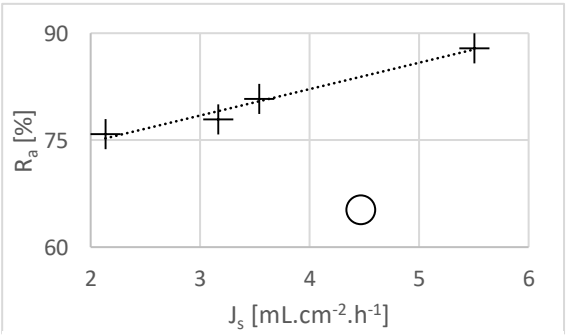

Figure 5 - Apparent rejection plotted against solvent flux of modular approach trials. A linear relationship can be seen in the data.

2.3.4. Final Modular approach

As a final approach, a new model was designed in order to aggregate the findings of this dissertation into a working prototype. To this effect, instead of relying on the support to make the binding connection between module and support, relying on the module part leads to the support pressing against the module instead of pressing away from it (Figure 5 – a; Figure 5 – b). This strengthens the connection considerably.

In addition, the ring was also modified. It was designed to surround the support, stopping it from sliding around during the gluing process, this way avoiding potential flaws during the gluing process that might have existed in different trials (Figure 5 – c).

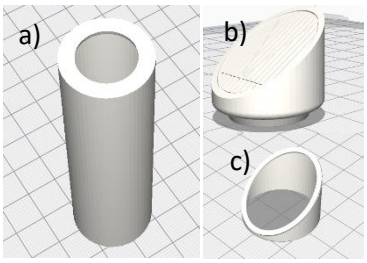

Figure 5 - Cura view of the new modular device a) Module part; b) Membrane support part, c) ring part.

When this device was tested with a NF membrane at pressure of 20 bar with a blue-250 solution, a similar flux was achieved to that of the average in section 2.3.2. The rejection, however, was of nearly 100%, with no discernible micro-leaks visible in the device. Altogether, this means this sealing method is at least capable of resisting the creation of micro-leaks and, allied to everything else, shows that performing centrifugal concentration of small samples is possible using this device.

2.4. Future considerations

Despite showing promising results, there is still much work that must be done on this project in order to make it commercially viable. In this final segment, I propose several improvements on the current model and suggest further testing based on the observations made throughout the development of this project

Firstly, the gluing must be optimized. This involves finding the perfect gluing area for the current cyanoacrylate gel. Tests should be performed for different module ring sizes larger and smaller than the current 2 mm. It should be kept in mind that the larger the ring, the smaller the active membrane area. This indirect relationship between gluing area and membrane area need to be carefully considered when performing these tests. Alternatively, exploration of a different adhesive all

together is possible. This adhesive should be able to hold PLA-PLA and PLA-membrane connections up to at least 30 bar without leakage for several sequential tests, even after the PLA becomes hydrated.

Secondly, test pertaining to the inner block should be performed. While empty chamber runs will be able to analyse fluxes and rejections properly enough to analyse if the device works, an inner piece that extends the height of the sample and minimizes the sample volume will effectively enhance the flux through the membrane (pressure remains higher for longer) and increase the CF vastly.

Moreover, tests to properly ascertain the concentrating capacities of the device should be performed, where CF is calculated for different osmotic pressure and pressure conditions.

After this, optimization of the β angle is mandatory. This angle is responsible for the self-cleaning effect and optimizing this angle will lead to the largest possible flux and lesser possible rejection in the device. For commercial applications, this translates into a better concentration factor for NF modules and membranes capable of concentrating most, if not all proteins without the addition of non-gelling agents for UF modules. Angles that allow for membranes to be dragged away from the membrane will give better results. In this particular model, these should correspond to $\beta < 0º$.

Other possible test would include, but not limited to: testing several solutes at once; testing fouling resistance; testing protein gelling layer resistance; testing the device for MF, UF and NF; testing different types of internal blocks.

Finally, a possible material and structure overhaul could be enforced. A more resilient shell could be designed in another material, with a detachable permeate chamber for easy cleaning and permeate recovery. The module itself could be extruded in PC rather than being printed in PLA. This would also optimize the gluing situation previously discussed, as PC is both smother and less hydratable than PLA, making it potentially better for membrane securing. Additionally, other plastics could be explored based on mechanical characteristics and economic viability. Even if it meant losing the fully disposable nature of the device, this proposal would not only massively improve the versatility of centrifugal filtration as a whole, by allowing the same device to be used for any purpose but would also reduce plastic waste in as much as 600% when considering the waste of a disposable device with the waste of a single module.

3. Conclusions

The main goal of this dissertation started out as being the development of a commercially viable device for batchwise centrifugal nanofiltration. As both the project and the device developed, the goal shifted to developing a commercially viable batchwise centrifugal filtration device capable of performing a range of operations, from large particle and colloid filtration (MF) to concentration of solutes with MW as low as $1000 g.mol^{-1}$ (NF).

Several different models were designed and prepared throughout this work. Apart from the outer PC shells and the membranes, all the pieces needed were printed in PLA and manufactured using a 3D printer and glued using different adhesive types. The devices were subjected to a multitude of tests that led to a final device being submitted as the main result of this thesis.

The device in question is a modular device capable of switching membrane modules in order to perform different types of operations with the same basic material. It is mainly intended to both perform nanofiltration of small samples (< 100 mL) and ultrafiltration of particularly difficult to process solutes, such as proteins which can't be filtered by conventional means because of high gel polarization.

Tested the model at an UF level with filtration runs using a 5 wt% solution of PEG35k showed results with fairly normal fluxes, with an average of 3.59 ± 0.05 $mL.cm^{-2}.h^{-1}$. The rejections, however, were a bit low. The expected values were of 100.0%, but the actual rejections averaged at 80.63 ± 0.02 % and peaked at 87.95 ± 0.03 %. These low rejections are explained by small fissures in the glue, either due to failure during the gluing process or to the intrinsic irregularity of a printed PLA surface. These fissures were fixed in later runs by restructuring the pressure points of the device and allowing for rejections of nearly 100% with NF runs.

The proposed device shows high promise in regard to the objectives laid out on the beginning of this dissertation. Because of the contributions of Completo et al. (2017) and Hams (2018), we know the device's general geometry to be able to highly concentrate low MW solute solutions at a small-volume scale. Due to the membrane position and high pressures and highly negative β angles

allowed by this device, non-saline protein treatment should show high mitigation of gel and concentration polarization. Furthermore, by applying the material overhaul discussed in section 2.4, not only can the device become more secure from a mechanical point of view, allowing any current problems to be surpassed, but it would also become less of an environmental and economic burden by reducing plastic consumption in as much as 600%.

All in all, the contraption created for this project shows capable of performing the tasks it aimed to perform and proposes an alternative to the currently used devices by not only performing the same tasks but achieving two entirely new task as yet impossible in most laboratory environments.

The following list summarizes the main conclusions found in this segment:

- A new, innovative prototype capable of performing centrifugal nanofiltration for the concentration of small-samples (<100 mL) and centrifugal ultrafiltration of small-samples of non-saline protein solutions without gel polarization was designed;
- Fluxes were limited only by the membranes used, with mass transport limitations including fouling, concentration polarization and gel-layer polarization being mitigated by the geometry of the device, which is able to achieve rejections of 100%;
- The modular approach facilitates retentate removal, assembly, switching separation processes and leads to less plastic waste.

7. References

Alfa Laval. 2019. 'Flat Sheet Membranes for Ultrafiltration — FS, UFX, RC and ETNA Types'. 23 September 2019. https://www.alfalaval.com/globalassets/documents/products/separation/membranes/flat-sheet-membranes/uf-flat-sheet-membranes_200000311-1-en-gb.pdf.

Ao, L., W. Liu, L. Zhao, and X. Wang. 2016. 'Membrane Fouling in Ultrafiltration of Natural Water after Pretreatment to Different Extents'. *Journal of Environmental Sciences* 43 (May): 234–43. DOI:10.1016/j.jes.2015.09.008

Baker, R.W. 2000. 'MEMBRANE SEPARATION'. In *Encyclopedia of Separation Science*, 189–210. Elsevier. DOI:10.1016/B0-12-226770-2/00101-0.

Barr, J., and L. White. 2006. 'Centrifugal Drum Filtration: I. A Compression Rheology Model of Cake Formation'. *AIChE J,* 52: 545–556. DOI:10.1002/aic.10678.

Blender (version 2.8). 2019. Netherlands: Blender Foundation. blender.org.

Carman, P.C. 1997. 'Fluid Flow through Granular Beds'. *Chemical Engineering Research and Design* 75 (December): S32–48. DOI:10.1016/S0263-8762(97)80003-2.

Completo, C., V. Geraldes, V. Semião, M. Mateus, and M. Rodrigues. 2017. 'Centrifugal Nanofiltration for Small-Volume Samples'. *Journal of Membrane Science* 540 (October): 411–21. DOI:10.1016/j.memsci.2017.06.069.

Filmtech. 2019. 'FILMTEC™ NF90 Nanofiltration Elements for Commercial Systems'. 23 September 2019. https://www.dupont.com/content/dam/dupont/amer/us/en/products/water-solutions/documents/609-00378.pdf.

Gordeev, E. G., A. S. Galushko, and V. P. Ananikov. 2018. 'Improvement of Quality of 3D Printed Objects by Elimination of Microscopic Structural Defects in Fused Deposition Modeling'. Edited by Michael C. McAlpine. *PLOS ONE* 13 (6): e0198370. DOI:10.1371/journal.pone.0198370.

Hams, S.. 2018. 'Development and Optimization of a Centrifugal Nanofiltration Device for Small Volume Samples Master-Thesis'. Lisboa: Technische Universität Dortmund & Instituto Superior Técnico.

Henkel. 2019. 'Technical Data Sheet: Loctite® Power Flex'. 18 September 2019. http://www.farnell.com/datasheets/1675708.pdf.

Hilal, N., O. O. Ogunbiyi, N. J. Miles, and R. Nigmatullin. 2005. 'Methods Employed for Control of Fouling in MF and UF Membranes: A Comprehensive Review'. *Separation Science and Technology* 40 (10): 1957–2005. DOI:10.1081/SS-200068409.

Kedem, O., and A. Katchalsky. 1961. 'A Physical Interpretation of the Phenomenological Coefficients of Membrane Permeability'. *The Journal of General Physiology* 45 (1): 143–79. DOI:10.1085/jgp.45.1.143.

Lenntech. 2001. ‘P3-Ultrasil-110’. 2001. https://www.lenntech.com/Data-sheets/ECOLAB-P3-ultrasil-110-L-EN.pdf.

Lewis, G. N.. 1908. ‘The Osmotic Pressure of Concentrated Solutions, and the Laws of the Perfect Solution’. *Journal of the American Chemical Society* 30 (5): 668–83. DOI:10.1021/ja01947a002.

Lipnizki, F. 2005. ‘Industrial Applications of Ultrafiltration in Pharmaceutical Biotechnology’. *Engineering in Life Sciences* 5 (1): 81–83. DOI:10.1002/elsc.200407047.

Luis, P.. 2018. ‘Introduction’. In *Fundamental Modelling of Membrane Systems*, 1–23. Elsevier. DOI:10.1016/B978-0-12-813483-2.00001-0.

Pacer Technology. 2019. ‘PRODUCT SALES SHEET: Z-Poxy™ 30Min System’. 17 September 2019. https://www.amcsupplies.com.au/manuals/Z-Poxy%2030%20Min%20System%20-%20TDS.pdf.

Pall Life sciences. 2003. ‘Centrifugal Devices for Ultrafiltration & Microfiltration Nanosep®, Microsep™, Macrosep®, and Jumbosep™ Devices’. 2003. http://wolfson.huji.ac.il/purification/PDF/dialysis/PALL_CentrifualDevice.pdf.

Porter, M. C., ed. 1990. *Handbook of Industrial Membrane Technology*. Park Ridge, N.J., U.S.A: Noyes Publications.

Present Onshape Inc. 2014. ‘Onshape | Product Development Platform’. 2014. https://www.onshape.com/.

Rudie, B. J., T. A. Torgrimson, and D. D. Spatz. 1985. ‘Reverse-Osmosis and Ultrafiltration Membrane Compaction and Fouling Studies Using Ultrafiltration Pretreatment’. In *Reverse Osmosis and Ultrafiltration*, edited by S. Sourirajan and Takeshi Matsuura, 281:403–14. Washington, D.C.: American Chemical Society. DOI:10.1021/bk-1985-0281.ch029.

Sigma-Aldrich. 2019a. ‘Coomassie® Brilliant Blue G 250 (C.I. 42655) CAS 6104-58-1 | 115444’. 2019. http://www.merckmillipore.com/PT/en/product/Coomassie-Brilliant-blue-G-250-C.I.-42655,MDA_CHEM-115444?ReferrerURL=https%3A%2F%2Fwww.google.com%2F.

Sigma-Aldrich. 2019b. ‘Poly(Ethylene Glycol) 35,000 | Sigma-Aldrich’. 2019. https://www.sigmaaldrich.com/catalog/product/aldrich/81310?lang=pt&region=PT.

Siparsky, G., K. Voorhees, J. Dorgan, and K. Schilling. 1997. ‘Water Transport in Polylactic Acid (PLA), PLA/ Polycaprolactone Copolymers, and PLA/Polyethylene Glycol Blends’. *Journal of Environmental Polymer Degradation* 5 (3): 125–36. DOI:10.1007/BF02763656.

Smartfill. 2019. ‘Smartfil PLA’. Accessed 17 September 2019. https://filament2print.com/gb/index.php?controller=attachment&id_attachment=13.

Stansbury, J. W., and M. J. Idacavage. 2016. ‘3D Printing with Polymers: Challenges among Expanding Options and Opportunities’. *Dental Materials* 32 (1): 54–64. DOI:10.1016/j.dental.2015.09.018.

Svarovsky, L. 2001. ‘Centrifugal Filtration’. In *Solid-Liquid Separation*, 432–41. Elsevier. DOI:10.1016/B978-075064568-3/50040-7.

Székely, G., M. Gil, B. Sellergren, W. Heggie, and F. C. Ferreira. 2013. ‘Environmental and Economic Analysis for Selection and Engineering Sustainable API Degenotoxification Processes’. *Green Chem.* 15 (1): 210–25. DOI:10.1039/C2GC36239B.

Thermo scientific. 2001. ‘NALGENE Centrifuge Tubes and Bottles’. 2001. catalogus.de/pdf/30/centrifugecatintl.pdf.

Thermo Scientific. 2019a. ‘Thermo Scientific Sorvall RC6 plus Superspeed Centrifuge’. 2019a. https://www.grupo-certilab.com/resources/files/S/CENTRIFUGAS/RC-6%20PLUS.PDF.

Thermo-Scientific. 2019b. ‘SA-300 Fixed Angle Rotor’. 2019b. https://www.thermofisher.com/order/catalog/product/18100#/18100.

Ultimaker Cura (version 4.3). 2019. https://ultimaker.com/software/ultimaker-cura.

Volkov, A. 2014. ‘Membrane Compaction’. In *Encyclopedia of Membranes*, 1st ed. Berlin: Springer-Verlag.